Durham University

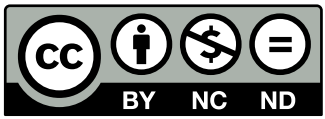
Mathematical aspects of the power-law discharge function used in rainfall-runoff modelling

Simon Mathias
Department of Engineering
Durham University



Citation: Mathias, S. A. (2026) Mathematical aspects of the power-law discharge function used in rainfall-runoff modelling. A seminar given at Bath University 10/11/2026. Durham University. https://samathiasuk.github.io/2026_Bath_Power_Law_Seminar/2026_Bath_Power_Law_Seminar.pdf

This work is licensed under a Creative Commons "Attribution-NonCommercial-NoDerivatives 4.0 International" license.



Contents

1 Introduction **4**

2 The master recession curve **5**

3 The power-law discharge function **7**

4 Physics-based values of b **8**
4.1 Laminar sheet flow approximation 8
4.2 Turbulent sheet flow approximation 10
4.3 Unconfined aquifer approximation 10
4.4 The exponential storage model 12

5 Behaviour during recession **13**

6 Analytical solutions **15**
6.1 Linear discharge function 15
6.2 Quadratic discharge function 16
6.3 Infinite power law discharge function 17

7 Euler explicit solution **18**
7.1 Stability analysis for Euler explicit schemes . . . 18
7.1.1 Development of a stability constraint . . 19
7.1.2 Application of a stability constraint . . . 20
7.1.3 A $q_{\max}$ formulation 21

8 Recession analysis examples **21**

9 Conclusions **26**

References **27**

Abstract

Power-law relationships between catchment storage and discharge are widely used in conceptual rainfall-runoff models and provide a simple means of representing nonlinear catchment response. Despite their apparent simplicity, these relationships have a number of interesting mathematical properties and can be interpreted in terms of several familiar hydraulic systems. This seminar explores the mathematical basis and practical implications of the power-law discharge function. The relationship with the master recession curve is first considered, before examining how different power-law exponents can arise from physical arguments based on Poiseuille flow, Manning's equation and groundwater drainage from an unconfined aquifer. The limiting behaviour of the power-law formulation as the power-law exponent tends to infinity is also explored through its relationship with the exponential storage model. Attention is then given to the solution of the resulting storage equations. Analytical solutions are presented for several special cases, alongside numerical solutions using explicit time-stepping. The stability constraints associated with explicit time-stepping are examined and used to motivate a maximum-discharge formulation that avoids numerical instability. Finally, it is shown how streamflow recessions can be isolated from observed river-flow data using a modified implementation of GR4J incorporating the PDM rainfall-runoff model. Linear regression of individual recession periods is then used to illustrate the range of power-law exponents inferred from catchment data and to consider what these values imply for the representation of nonlinear storage-discharge behaviour in rainfall-runoff models.

Learning outcomes

- Derive physically based values of the power-law exponent b for different flow systems.
- Relate the power-law discharge function to river-flow recession behaviour.
- Derive analytical solutions for selected values of the power-law exponent b.
- Derive and apply a stability constraint for an Euler explicit routing scheme.
- Determine b values from observed recession data.

Notation

a	Empirical coefficient for river flow routing function [$L^{1-b}T^{-1}$].
A	Catchment area [L^2].
b	Empirical exponent for river flow routing function [-].
B	Breadth of an unconfined aquifer [L].
g	Gravitational acceleration [LT^{-2}].
h	Water depth or water table elevation above an impermeable base [L].
L	Length of an unconfined aquifer [L].
m	Hydraulic radius [L].
n	Manning's coefficient [$L^{-1/3}T$].
P	Wetted perimeter [L].
q	River flow rate per unit area of catchment [LT^{-1}].
$q_{\max}$	Maximum stable value of q [LT^{-1}].
q_s	Net rainfall [LT^{-1}].

Q River flow rate [L^3T^{-1}].

s Dummy variable for studying numerical stability [-].

t Time [T].

Δt Time-step duration [T].

v Volume of water stored within the river channel network per unit area of catchment [L].

v_{max} Maximum stable value of v [L].

v_{trial} Trial value of v [L].

V Volume of water stored within the river channel network [L^3].

w Dummy variable for studying numerical stability [T^{-1}].

w Uniform recharge rate [LT^{-1}].

α Empirical coefficient for the river flow routing function [$L^{\frac{1}{b}-1}T^{-\frac{1}{b}}$].

β Empirical exponent for the river flow routing function [-].

ε Error term for studying numerical stability [-].

μ Dynamic viscosity [$ML^{-1}T^{-1}$].

ρ Density of water [ML^{-3}].

1 Introduction

Conceptual rainfall–runoff models commonly represent the release of water from catchment storage using relatively simple mathematical functions. One of the most general is the power-law discharge relationship $q = av^b$ where q is the river flow rate per unit catchment area, v is the corresponding volume of stored water per unit area, and a and b are empirical parameters. The special case $b = 1$ corresponds to the familiar linear reservoir, while values of $b \neq 1$ allow the rate of drainage to vary non-linearly with catchment storage. Despite its apparent simplicity, the power-law discharge function has a number of interesting

mathematical and physical properties. Different values of the exponent b can be related to different idealised hydraulic systems, while the same formulation leads directly to a power-law description of river-flow recession. The choice of b also influences the analytical form of the resulting rainfall–runoff model and, when the governing equations are solved numerically, its stability. The purpose of this seminar is to explore these properties and their implications for rainfall–runoff modelling.

We begin with the traditional master recession curve and use it to establish the relationship between storage–discharge behaviour and river-flow recession. We then investigate physically based interpretations of the power-law exponent using idealised surface-water and groundwater systems. Analytical and numerical solutions of the resulting storage equation are subsequently considered, including the stability constraints associated with explicit time-stepping and the resulting concept of a maximum stable discharge. Finally, recession data from four UK catchments are used to examine the extent to which the theoretical behaviour is reflected in observed river flows.

2 The master recession curve

The master recession curve represents a traditional approach to analysing river flow data, Q [$\mathrm{L^3T^{-1}}$]. The basic process involves plotting an annual cycle of river-flow time-series data on a logarithmic scale, identifying significant recession events, and shifting these backwards in time such that the recession limbs approximately align along a single straight line on a log-linear plot (see Fig. 1). This straight line represents an equation of the form

$$Q = Q_0 \exp\left(-\frac{t}{T}\right) \tag{1}$$

where Q_0 [ML^{-3}] represents an initial discharge, t [T] is time and T [T] is thought to represent the residence time of the catchment.

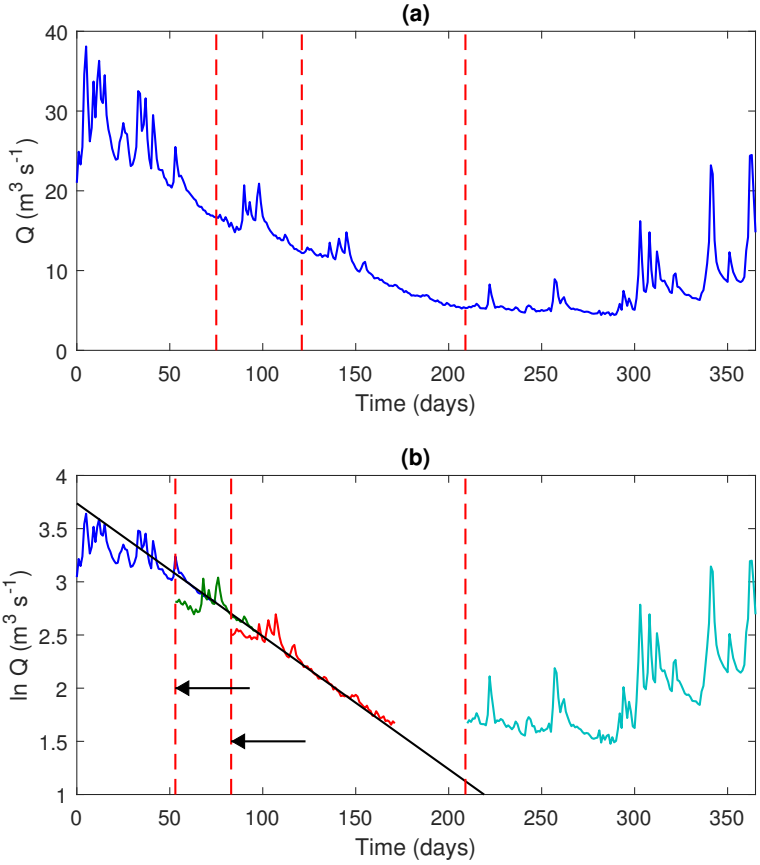


Figure 1: Schematic example showing how a master recession curve is constructed. In this case the master recession curve (the black solid line) is $Q = 42\exp(-t/80)$.

Differentiating Eq. (1) with respect time and substituting Eq. (1) back into the resulting expression gives

$$\frac{dQ}{dt} = -\frac{Q}{T} \tag{2}$$

which describes the recession of a linear reservoir. This line of reasoning provides an empirical basis for the widespread use of linear-reservoir equations in rainfall-runoff models. However, as we will explore in more detail, neither empirical observations nor theoretical considerations provide particularly strong support for the assumption that catchment recession should generally follow linear-reservoir behaviour.

3 The power-law discharge function

Let V [L^3] be the volume of water stored within a river channel network and Q [L^3T^{-1}] be the river flow rate at the catchment outlet. Mass conservation dictates that

$$\frac{dV}{dt} = Aq_s - Q \tag{3}$$

where q_s [LT^{-1}] is the net rainfall landing over catchment (i.e., rainfall minus actual evapotranspiration) and A [L^2] is the catchment area.

It is convenient to normalise the above equation by dividing both sides by the catchment area to get

$$\frac{dv}{dt} = q_s - q \tag{4}$$

where $v = V/A$ and $q = Q/A$.

It can be understood that the dryer the catchment is, the smaller the flow rate out of the catchment. A simple but general empirical relationship to consider is [5, p. 462]

$$q = av^b \tag{5}$$

where a [$L^{1-b}T^{-1}$] and b [-] are empirical coefficients yet to be defined.

4 Physics-based values of b

It is possible to demonstrate that different values of b imply different physical ideas. For example, $b = 1$ implies that the river behaves in the same way as a linear reservoir. Below we will look at four more possibilities including laminar sheet flow, turbulent sheet flow, unconfined aquifer flow and exponential storage flow.

4.1 Laminar sheet flow approximation

Imagine water flows as a sheet across the catchment with a uniform thickness, h [L]. A corresponding value of the exponent, b, can be determined under laminar and turbulent flow conditions.

Under steady laminar flow conditions, the flow rate can be determined from the Poiseuille equation [5, p. 50]

$$Q = \frac{\rho g A_c m^2 S_0}{c_0 \mu} \tag{6}$$

where A_c [L^2] is the flowing cross-sectional area of the river channel, $m = A_c/P$ [L] is the hydraulic radius, P is the wetted perimeter [L], S_0 [-] is the slope of the river bed, ρ [ML^{-3}] is the fluid density, g [LT^{-2}] is gravitational acceleration, μ [$ML^{-1}T^{-1}$] is the dynamic viscosity and $c_0 \in [2,3]$ [-] is a dimensionless geometrical factor. The dimensions of the channel are further illustrated in Fig. 2.

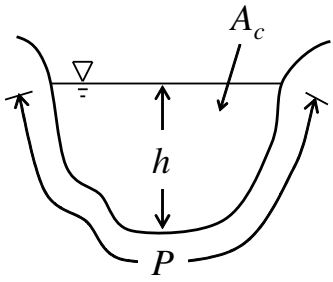


Figure 2: Schematic diagram of the river channel model.

Challenge 1. Use the Poiseuille equation to derive expressions for the power law coefficients in Eq. (5) in terms of wetted perimeter, slope, catchment area, geometrical factor, density, gravitational acceleration, and dynamic viscosity.

The total volume of water in the sheet, $V = Ah$. It follows that $h = V/A = v$. The flowing cross-sectional area of the catchment is found from $A_c = Ph = Pv$ where P [L] is the wetted perimeter of the flowing channel. Furthermore, the hydraulic radius, $m = A_c/P = v$.

Substituting the above expressions into Eq. (6) leads to [4]

$$q = \frac{\rho g P S_0 v^3}{A c_0 \mu} \tag{7}$$

Comparing Eq. (7) with Eq. (5) then suggests that [5, p. 462]

$$a = \frac{\rho g P S_0}{A c_0 \mu} \quad \text{and} \quad b = 3$$

4.2 Turbulent sheet flow approximation

Under turbulent flow conditions Manning's equation can be used where [5, p. 51]

$$Q^2 = \frac{A_c^2 m^{4/3} S_0}{n^2} \tag{8}$$

and n [$L^{-1/3}T$] is Manning's coefficient.

Challenge 2. Use Manning's equation to derive expressions for the power law coefficients in Eq. (5) in terms of wetted perimeter, slope, catchment area and Manning's coefficient.

Again, $A_c = Pv$ and $m = A_c/P = v$.

Substituting the above expressions into Eq. (8) leads to [4]

$$q = \frac{PS_0^{1/2} v^{5/3}}{An} \tag{9}$$

Comparing Eq. (9) with Eq. (5) then suggests that [5, p. 463]

$$a = \frac{PS_0^{1/2}}{An} \quad \text{and} \quad b = \frac{5}{3}$$

4.3 Unconfined aquifer approximation

Consider a one-dimensional unconfined aquifer of length, L [L], and breadth, B [L], with hydraulic conductivity, K [LT^{-1}], and subject to a steady, spatially uniform recharge rate, W [LT^{-1}] (see Fig. 3a). If the water table elevation above the impermeable base, h [L], is fixed at $h = h_0$ at $x = 0$ and $x = L$, then, under the Dupuit approximation [5, p. 308]

$$h^2 = h_0^2 + \frac{Wx}{K}(L - x) \tag{10}$$

and the groundwater discharge flow across a section at position, x, is

$$Q = BW\left(x - \frac{L}{2}\right) \tag{11}$$

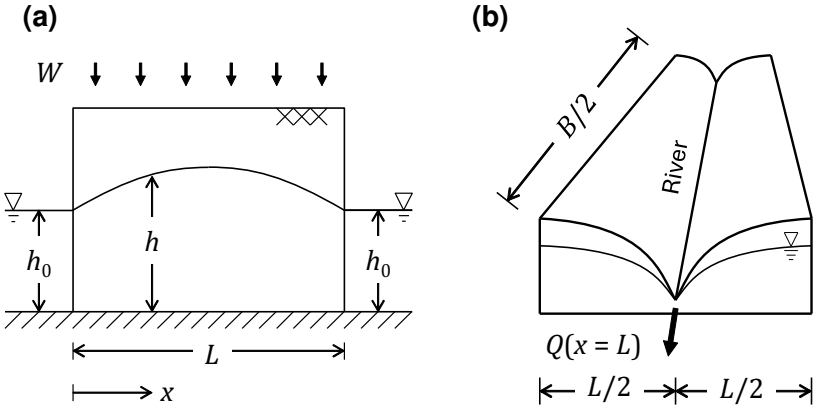


Figure 3: Schematic diagrams for the unconfined aquifer flow assumption.

Suppose we cut the aquifer in half along the line $x = L/2$. We then take one half and fold it such that the $h = h_0$ boundary is folded in on itself, so that it now represents a river of length $B/2$, while the surrounding unconfined aquifer represents its catchment (see Fig. 3b). In this case, $Q(x = L) = BWL/2$ represents the total flow rate out of the river at the catchment outlet.

For an aquifer with a specific yield, S_y [-], the drainable vol-

ume of water stored in the catchment, V, is found from

$$\begin{aligned} V &= S_y B \int_0^{L/2} h dx \\ &= S_y B \int_0^{L/2} \left[h_0^2 + \frac{Wx}{K}(L-x) \right]^{1/2} dx \\ &= S_y BL \left(\frac{W}{K} \right)^{1/2} \int_0^{L/2} \left[\varepsilon + \frac{x}{L}\left(1 - \frac{x}{L}\right) \right]^{1/2} dx \\ &= \frac{\pi S_y BL^2}{16} \left(\frac{W}{K} \right)^{1/2} + O(\varepsilon) \end{aligned} \tag{12}$$

where

$$\varepsilon = \frac{Kh_0^2}{WL^2} \tag{13}$$

The area of the catchment, $A = BL/2$. Therefore the flow per unit area, $q = W$, and the volume per unit area

$$v = \frac{V}{A} = \frac{\pi S_y L}{8} \left(\frac{q}{K} \right)^{1/2} + O(\varepsilon) \tag{14}$$

whence [2]

$$q = \frac{64Kv^2}{(\pi S_y L)^2} \tag{15}$$

Comparing Eq. (15) with Eq. (5) then suggests that

$$a = \frac{64K}{(\pi S_y L)^2} \quad \text{and} \quad b = 2$$

4.4 The exponential storage model

Solving Eq. (5) for v leads to

$$v = \left(\frac{q}{a} \right)^{\frac{1}{b}} \tag{16}$$

Differentiating Eq. (16) with respect to q yields

$$\frac{\partial v}{\partial q} = \frac{q^{\frac{1}{b}-1}}{\alpha} \tag{17}$$

where

$$\alpha = a^{\frac{1}{b}} b \tag{18}$$

When $b \to \infty$

$$\lim_{b\to\infty} \frac{\partial v}{\partial q} = \frac{1}{\alpha q} \tag{19}$$

Integrating Eq. (19) with respect to v leads to

$$v = \frac{1}{\alpha} \ln q + C \tag{20}$$

whence [9]

$$q = B \exp(\alpha v) \tag{21}$$

where

$$B = \exp(-\alpha C) \tag{22}$$

The derivation of Eq. (21) shows that it is possible to define the response of the power law discharge function where the exponent is infinite. It corresponds to an exponential storage model

5 Behaviour during recession

When the contribution to the river is zero (i.e., $q_s = 0$), the river is said to be in recession. Whilst the above analysis has provided some simple ideas about likely values of the power law exponent, b, the sheet flow assumption is quite unrealistic, and both a and b are better found by calibration against observed river flow rates [6]. Nevertheless, further insight into the meaning of a and b can be gained by studying how the above model behaves during recession events.

Challenge 3. Use Eqs. (4) and (5) to determine a relationship between $\frac{dq}{dt}$ and q when $q_s = 0$.

Applying the chain rule to Eq. (4) leads to

$$\frac{\partial v}{\partial q}\frac{dq}{dt} = q_s - q \tag{23}$$

Solving Eq. (5) for v gives us

$$v = \left(\frac{q}{a}\right)^{\frac{1}{b}} \tag{24}$$

Differentiating Eq. (24) with respect to q leads to

$$\frac{\partial v}{\partial q} = \frac{q^{\frac{1}{b}-1}}{a^{\frac{1}{b}}b} \tag{25}$$

Substituting Eq. (25) into Eq. (23) gives us

$$\frac{dq}{dt} = a^{\frac{1}{b}}bq^{1-\frac{1}{b}}(q_s - q) \tag{26}$$

During a recession event $q_s = 0$ so [5, p.464]

$$\frac{dq}{dt} = -\alpha q^{\beta} \tag{27}$$

where

$$\alpha = a^{\frac{1}{b}}b \quad \text{and} \quad \beta = 2 - \frac{1}{b}$$

from which it can be understood that during a recession event, $\frac{dq}{dt}$ is a power law of q with β being its exponent. Note that $\lim_{b\to\infty} \beta = 2$.

6 Analytical solutions

From Eq. (26) we have

$$\frac{dq}{dt} = \alpha q^{1-\frac{1}{b}}(q_s - q) \tag{28}$$

Over a finite time increment, δt, $t \to t + \delta t$ and $q \to q + \delta q$. Separating variables in Eq. (28) and integrating over these intervals gives

$$\alpha \delta t = \int_q^{q+\delta q} \frac{1}{q^{1-\frac{1}{b}}(q_s - q)} dq \tag{29}$$

The mean change in flow rate during the interval $[t, t + \Delta t]$ is obtained from

$$\langle \Delta q \rangle = \frac{1}{\Delta t} \int_0^{\Delta t} \delta q d\delta t \tag{30}$$

Assuming that q_s is constant over the interval $[t, t + \Delta t]$, the associated mean daily discharge for this period is calculated as $q + \langle \Delta q \rangle$, where q represents the instantaneous discharge rate at time, t. The instantaneous discharge rate at time, $t + \Delta t$, is obtained from $q + \Delta q$, where $\Delta q = \delta q(\delta t = \Delta t)$. This updated rate, $q + \Delta q$, can be used to calculate $\langle \Delta q \rangle$ for a next time-step Mathias et al. [7].

It is possible to determine closed form and exact expressions for Δq and $\langle \Delta q \rangle$ for three special cases, when $b = 1$, $b = 2$ and $b \to \infty$.

6.1 Linear discharge function

When $b = 1$, $q = av$ and Eq. (29) leads to [1]

$$\alpha \delta t = \ln \left(\frac{q_s - q}{q_s - q - \delta q} \right) \tag{31}$$

Solving Eq. (31) for δq gives us

$$\delta q = (q_s - q)[1 - \exp(-\alpha \delta t)] \tag{32}$$

whence

$$\Delta q = (q_s - q)[1 - \exp(-\alpha \Delta t)] \tag{33}$$

and substituting Eq. (32) into Eq. (30) leads to

$$\begin{aligned} \langle \Delta q \rangle &= \frac{1}{\Delta t} \left\{ (q_s - q) \left[\delta t + \frac{e^{-\alpha \delta t}}{\alpha} \right] \right\}_0^{\Delta t} \\ &= q_s - q - \frac{\Delta q}{\alpha \Delta t} \end{aligned} \tag{34}$$

6.2 Quadratic discharge function

When $b = 2$, $q = av^2$ and Eq. (29) leads to [1]

$$\alpha \delta t = \frac{2}{\sqrt{q_s}} \left[\operatorname{arctanh}\left(\sqrt{\frac{q+\delta q}{q_s}} \right) - \operatorname{arctanh}\left(\sqrt{\frac{q}{q_s}} \right) \right] \tag{35}$$

Solving Eq. (35) for δq gives us

$$\delta q = q_s \tanh^2 \left[\frac{\alpha \delta t \sqrt{q_s}}{2} + \operatorname{arctanh}\left(\sqrt{\frac{q}{q_s}} \right) \right] - q \tag{36}$$

whence

$$\Delta q = q_s \tanh^2 \left[\frac{\alpha \Delta t \sqrt{q_s}}{2} + \operatorname{arctanh}\left(\sqrt{\frac{q}{q_s}} \right) \right] - q \tag{37}$$

and substituting Eq. (36) into Eq. (30) leads to

$$\begin{aligned} \langle \Delta q \rangle &= \frac{1}{\Delta t} \left\{ (q_s - q)\delta t - \frac{2\sqrt{q_s}}{\alpha} \tanh \left[\frac{\alpha \delta t \sqrt{q_s}}{2} + \operatorname{arctanh}\left(\sqrt{\frac{q}{q_s}} \right) \right] \right\}_0^{\Delta t} \\ &= q_s - q - \frac{2}{\alpha \Delta t} \left(\sqrt{q + \Delta q} - \sqrt{q} \right) \end{aligned} \tag{38}$$

Furthermore, given

$$\tanh(A+B) = \frac{\tanh A + \tanh B}{1 + \tanh A \tanh B} \tag{39}$$

it follows that

$$\Delta q = \left\{ \frac{\sqrt{q} + \sqrt{q_s} \tanh\left[\frac{\alpha \Delta t \sqrt{q_s}}{2}\right]}{1 + \sqrt{\frac{q}{q_s}} \tanh\left[\frac{\alpha \Delta t \sqrt{q_s}}{2}\right]} \right\}^2 - q \tag{40}$$

and

$$\lim_{q_s \to 0} \Delta q = q \left[\left(1 + \frac{\alpha \Delta t \sqrt{q}}{2} \right)^{-2} - 1 \right] \tag{41}$$

which is needed to simulate time-steps when $q_s = 0$.

6.3 Infinite power law discharge function

When $b \to \infty$, $q = av^{\infty}$ and Eq. (29) leads to [9]

$$\alpha \delta t = \frac{1}{q_s} \ln \left(\frac{1 - \frac{q_s}{q}}{1 - \frac{q_s}{q + \delta q}} \right) \tag{42}$$

Solving Eq. (42) for δq gives us

$$\delta q = \frac{q_s q}{q + (q_s - q) \exp(-q_s \alpha \delta t)} - q \tag{43}$$

whence

$$\Delta q = \frac{q_s q}{q + (q_s - q) \exp(-q_s \alpha \Delta t)} - q \tag{44}$$

and substituting Eq. (44) into Eq. (30) gives us

$$\begin{aligned} \langle \Delta q \rangle &= \left\{ \frac{(q_s - q)\delta t + \frac{1}{\alpha} \ln\left[q + (q_s - q) e^{-q_s \alpha \delta t}\right]}{\Delta t} \right\}_0^{\Delta t} \\ &= q_s - q - \frac{1}{\alpha \Delta t} \ln\left(\frac{q + \Delta q}{q}\right) \end{aligned} \tag{45}$$

Note that

$$\lim_{q_s \to 0} \Delta q = -\frac{\alpha q^2 \Delta t}{\alpha q \Delta t + 1} \tag{46}$$

which is needed to simulate time-steps when $q_s = 0$.

7 Euler explicit solution

Estimates of river flow rate per unit area of catchment at the catchment outlet, q, can be obtained for a given set of river flow contribution data, q_s, by numerical solution of Eq. (4). An Euler explicit solution for the river channel storage per unit area of catchment, v, takes the form

$$v_{i+1} \approx v_i + \Delta t (q_{s,i} - q_i) \tag{47}$$

where $v_{i+1} = v(t_i + \Delta t)$, $v_i = v(t_i)$, $q_{s,i} = q_s(t_i)$ and $q_i = q(t_i)$.

7.1 Stability analysis for Euler explicit schemes

Consider a differential equation of the form

$$\frac{ds}{dt} = -w \tag{48}$$

Applying an Euler explicit time-stepping scheme leads to a discrete solution of the form

$$s_{i+1} = s_i - \Delta t w_i \tag{49}$$

where $\Delta t = t_{i+1} - t_i$.

The approximate solution, $s(t_i) = s_i$, is related to an exact solution, s_0, by

$$s = s_0 + \varepsilon \tag{50}$$

where ε is the error associated with the approximation.

Substituting Eq. (50) into Eq. (48) leads to

$$\frac{ds_0}{dt} + \frac{d\varepsilon}{dt} = -w(s_0 + \varepsilon)$$

and applying a Taylor series expansion to $w(s_0 + \varepsilon)$ gives us

$$\frac{ds_0}{dt} + \frac{d\varepsilon}{dt} = -w(s_0) - \varepsilon\frac{\partial w}{\partial s_0} + O(\varepsilon^2) \tag{51}$$

Recalling that s_0 satisfies Eq. (48) exactly, Eq. (51) reduces to

$$\frac{d\varepsilon}{dt} = -\varepsilon\frac{\partial w}{\partial s_0} + O(\varepsilon^2) \tag{52}$$

Applying an Euler explicit time-stepping scheme to Eq. (52) and rearranging then leads to

$$\frac{\varepsilon_{i+1}}{\varepsilon_i} = 1 - \Delta t \left[\frac{\partial w}{\partial s_0}\right]_i + O(\varepsilon_i)$$

from which it can be understood that Eq. (49) will remain stable providing [6]

$$\frac{\partial w}{\partial s} < \frac{1}{\Delta t} \tag{53}$$

7.1.1 Development of a stability constraint

Challenge 4. Compare Eqs. (4) and (48) and use Eq. (53) to derive an expression for the maximum stable value of v in terms of a, b and Δt.

Given Eqs. (4) and (53) and noting that $\partial q_s/\partial v = 0$, a stability constraint for our routing function can be obtained by imposing

$$\frac{\partial q}{\partial v} < \frac{1}{\Delta t}$$

Given $q = av^b$, it follows that stability should be ensured providing

$$abv^{b-1} < \frac{1}{\Delta t} \tag{54}$$

So the maximum stable value of v is found from [6]

$$v_{\max} = (ab\Delta t)^{\frac{1}{1-b}} \tag{55}$$

7.1.2 Application of a stability constraint

To force the stability criterion in Eq. (54) we can impose that $v < v_{\max}$ where $v_{\max} = (ab\Delta t)^{\frac{1}{1-b}}$, which can be achieved as follows [6]:

Consider the auxiliary variables, q_{trial} [LT^{-1}] and v_{trial} [L], found from

$$q_{\text{trial}} = av_i^b \quad \text{and} \quad v_{\text{trial}} = v_i + \Delta t(q_{s,i} - q_{\text{trial}}) \tag{56}$$

The $v_{\max}$ constraint can be applied by calculating q_i from

$$q_i = \begin{cases} q_{\text{trial}}, & v_{\text{trial}} < v_{\max} \\ q_{s,i} - \dfrac{(v_{\max} - v_i)}{\Delta t}, & v_{\text{trial}} \geq v_{\max} \end{cases} \tag{57}$$

and v_{i+1} from

$$v_{i+1} = \begin{cases} v_{\text{trial}}, & v_{\text{trial}} < v_{\max} \\ v_{\max}, & v_{\text{trial}} \geq v_{\max} \end{cases} \tag{58}$$

In this way, stability is ensured by routing excess river flow contribution direct to the catchment outlet during exceptionally wet periods.

7.1.3 A $q_{\max}$ formulation

The development and application of a stability constraint in Sections 7.1.1 and 7.1.2 points towards an alternative formulation for the non-linear routing function model defined by Eqs. (4) and (5). Let $q_{\max}$ [LT^{-1}] be the threshold value of q_s beyond which q_s bypasses the routing function directly to the catchment outlet as in Eq. (57). Substituting Eq. (55) into Eq. (5) suggests that

$$q_{\max} = a v_{\max}^{b} = a^{\frac{1}{1-b}} (b\Delta t)^{\frac{b}{1-b}} = (\alpha \Delta t)^{\frac{1}{1-\beta}} \tag{59}$$

Substituting Eq. (59) into Eq. (26) and implementing the threshold concept defined above leads to [5, p. 466]

$$\frac{dq}{dt} = \begin{cases} \frac{1}{\Delta t} \left(\frac{q}{q_{\max}} \right)^{1-\frac{1}{b}} (q_s - q), & q_s < q_{\max} \\ \frac{dq_s}{dt}, & q_s \geq q_{\max} \end{cases} \tag{60}$$

The $q_{\max}$ formulation is useful because it replaces the less intuitive parameter a with a flow rate that can be interpreted as a threshold above which water bypasses the routing store and passes directly to the catchment outlet. However, $q_{\max}$ is not a purely physical catchment property because its value depends on the choice of time-step, Δt. Consequently, changing the temporal resolution of the model also changes the value of $q_{\max}$.

8 Recession analysis examples

In this section, recession data are used to quantify values of α and β for four UK catchments, summary characteristics of which are listed in Table 1. Catchment-averaged rainfall and potential evapotranspiration data were obtained for each catchment from CAMELS-GB [3]. The associated river flow rates were obtained directly from the NRFA [10], because the precision of the flow-rate data stored in CAMELS-GB is insufficient for analysing the

low flows considered here. The four catchments were selected because they have broadly comparable catchment areas but substantially different baseflow indices (BFI).

Table 1: Summary information about the four river flow gauging stations selected for recession analysis.

Gauging station	(a) 80001	(b) 54018	(c) 55014	(d) 43005
Location	Dalbeattie	Hookagate	Byton	Amesbury
River	Urr	Rea Brook	Lugg	Avon
Catchment area (km^2)	197	173	203	326
CEH Baseflow Index (BFI) (-)	0.36	0.52	0.65	0.91
Mean annual precipitation (mm)	1427	774	1037	781
Mean annual potential evapotranspiration (mm)	475	500	496	518
Percentage urban land cover (%)	0.90	2.54	1.18	3.40

Recession data were identified using the rainfall–runoff model GR4Jb [7]. The model was calibrated against observations from 2005 to 2010 and subsequently used to estimate net rainfall, q_s, over the period from 2000 to 2015. Flow data corresponding to $q_s > 0.1$ mm day^{-1} were excluded, thereby restricting the analysis to periods with negligible net rainfall. The quantity q_s, referred to as Q_c in [7], is calculated within GR4Jb using a special case of the probability distributed model (PDM) [8]. For each pair of successive recession observations, values of $(dq/dt)_i$ and the corresponding midpoint discharge, q_i, were estimated using

$$\left(\frac{dq}{dt}\right)_i = \frac{q_n - q_{n-1}}{t_n - t_{n-1}} \quad \text{and} \quad q_i = \frac{q_n + q_{n-1}}{2} \tag{61}$$

The resulting recession data were then used to compare three parameterisations of the recession relationship given by Eq. (27). The first was obtained from the calibrated GR4Jb model, which assumes $\beta = 2$. The other two were obtained directly from the recession data by linear regression of

$$\ln\left[-\left(\frac{dq}{dt}\right)_i\right] = \ln\alpha + \beta \ln q_i \tag{62}$$

For the first regression, both α and β were treated as free parameters, whereas for the second, β was fixed to one, corresponding to the linear reservoir model.

Associated results for the four catchments are shown in Figs. 4, 5, 6 and 7. Subplots (a) compare the river flows simulated by GR4Jb with the observed river flows for the validation period from 2010 to 2015. The validation Nash–Sutcliffe Efficiency (NSE) values for all four catchments are greater than 0.833, indicating good agreement between the simulated and observed flows. Subplots (b) show the corresponding values of net rainfall, while subplots (c) identify the flow data subsequently selected for the recession analysis. Finally, subplots (d) compare the three different recession curves.

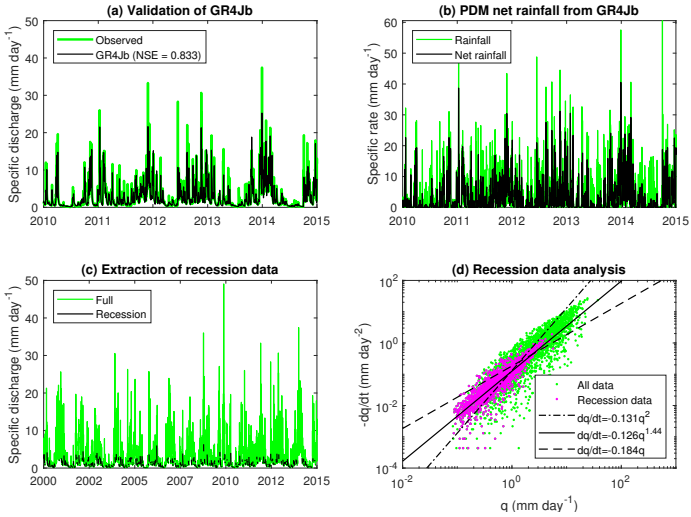


Figure 4: Recession analysis for River Urr at Dalbeattie.

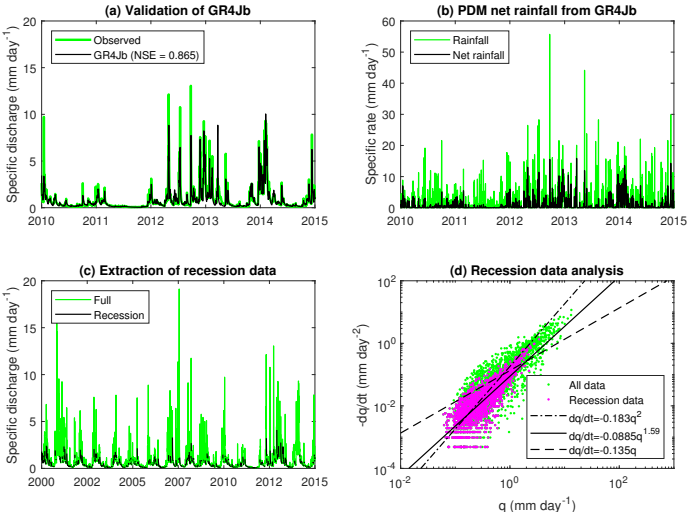


Figure 5: Recession analysis for River Rea Brook at Hookagate.

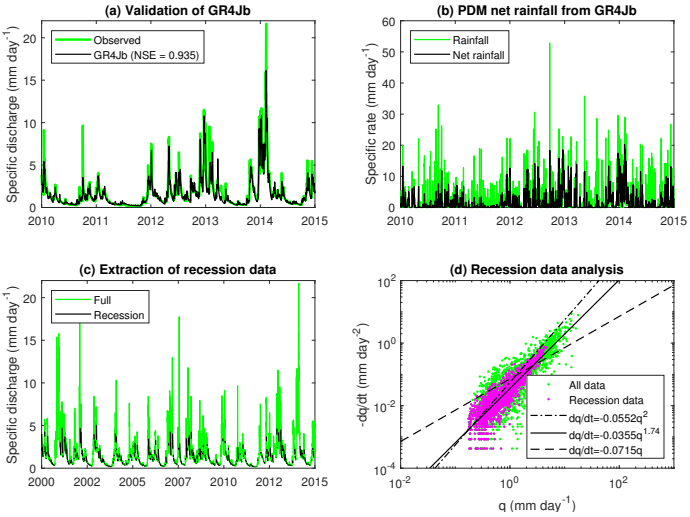


Figure 6: Recession analysis for River Lugg at Byton.

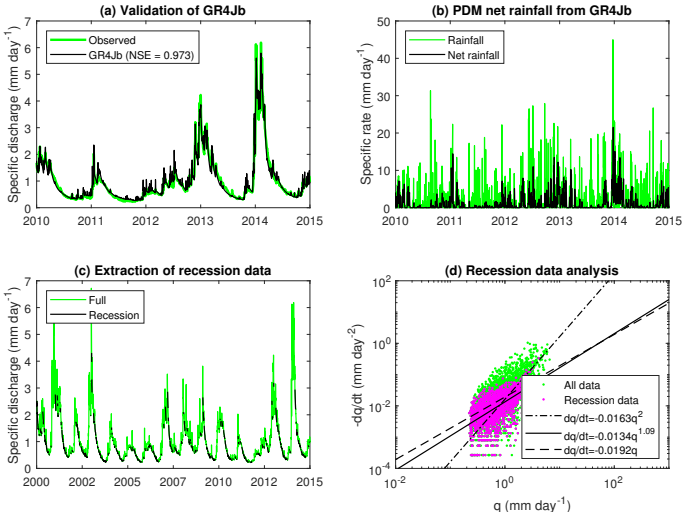


Figure 7: Recession analysis for River Avon at Amesbury.

Table 2: Summary results from recession analysis of data from the four river flow gauge stations listed in Table 1.

Gauge	BFI (-)	GR4Jb calibration		Regression analysis			
		α	q_{max} (mm day^{-1})	α	β (-)	b (-)	q_{max} (mm day^{-1})
80001	0.36	0.131	7.63	0.126	1.44	1.79	111
54018	0.52	0.183	5.46	0.0885	1.59	2.44	60.9
55014	0.65	0.0552	18.1	0.0355	1.74	3.85	91.0
43005	0.91	0.0163	61.3	0.0134	1.09	1.10	6.46E+20

Summary results are presented in Table 2. For the GR4Jb calibration, there is a systematic decrease in α and corresponding increase in q_{max} with increasing BFI. A broadly similar decrease in α is obtained from the regression analysis. The fitted values of β also increase approximately with BFI for the first three catchments, but this trend does not extend to Gauge 43005, which has the highest BFI of 0.91. Consequently, q_{max} does not

exhibit a systematic relationship with BFI when β is treated as a free parameter. This partly reflects the strong cross-correlation between fitted values of α and β, previously demonstrated by [6], but also the strong sensitivity of $q_{\max}$ to β as β approaches one (Eq. 59). This latter effect is particularly evident for Gauge 43005, for which $\beta = 1.09$ and the resulting value of $q_{\max}$ becomes extremely large.

9 Conclusions

The power-law discharge function provides a simple framework for representing non-linear storage–discharge behaviour in conceptual rainfall–runoff models, but its simplicity conceals a surprisingly rich range of behaviour. The analysis presented here has shown that the exponent b can be given a physical interpretation, with different idealised hydraulic systems leading naturally to different values of b. During periods of recession, the same storage–discharge relationship leads to the power-law recession equation $dq/dt = -\alpha q^{\beta}$ where $\beta = 2 - 1/b$, providing a direct connection between the internal structure of a rainfall–runoff model and recession behaviour that can be observed in river-flow data. The choice of power-law exponent also has important mathematical and numerical consequences.

Exact analytical solutions are available for several special cases, while explicit numerical solutions become increasingly constrained by stability as the non-linearity of the storage–discharge relationship increases. This stability constraint leads naturally to the definition of $q_{\max}$, which provides an intuitive means of limiting the routing store, although its dependence on the model time step means that it should not be interpreted as a purely physical catchment property. Analysis of four UK catchments demonstrates that recession behaviour can depart substantially from the

linear-reservoir assumption and that fitted power-law exponents vary between catchments. At the same time, the strong dependence between the fitted parameters α and β, together with the sensitivity of derived quantities such as $q_{\max}$ when β approaches one, cautions against assigning a simple physical interpretation to individual fitted parameter values.

References

[1] P. L. Bentura and C. Michel. Flood routing in a wide channel with a quadratic lag-and-route method. *Hydrological Sciences Journal*, 42:169–189, 1997.

[2] W. Brutsaert and J.L. Nieber. Analysis of flow processes in fractured chalk under pumped and ambient conditions (uk). *Water Resources Research*, 13:637–643, 1977.

[3] G. Coxon, N. Addor, J.P. Bloomfield, J. Freer, M. Fry, J. Hannaford, and et al. CAMELS-GB: hydrometeorological time series and landscape attributes for 671 catchments in great britain. *Earth Syst. Sci. Data*, 12(4):2459–2483, 2020.

[4] R. E. Horton. Erosional development of streams and their drainage basins. *Geol. Soc. Am. Bull.*, 56:275–370, 1945.

[5] S. A. Mathias. *Hydraulics, Hydrology and Environmental Engineering*. Springer, 2023. URL https://doi.org/10.1007/978-3-031-41973-7.

[6] S. A. Mathias, N. McIntyre, and R. H. Oughton. A study of non-linearity in rainfall-runoff response using 120 uk catchments. *Journal of Hydrology*, 540:423–436, 2016.

[7] S. A. Mathias, C. Thébault, and A. Ireson. A theoretical appraisal of the GR4J rainfall-runoff modelling framework. *Journal of Hydrology*, 664:134393, 2026.

[8] R. J. Moore. The pdm rainfall-runoff model. *Hydrology and Earth System Sciences*, 11(1):483–499, 2007.

[9] R. J. Moore and V. A. Bell. Incorporation of groundwater losses and well level data in rainfall-runoff models illustrated using the pdm. *Hydrology and Earth System Sciences*, 6(1):25–38, 2002.

[10] NRFA. *National River Flow Archive*. UK Centre for Ecology & Hydrology, 2023. URL https://nrfa.ceh.ac.uk/.